J. Cell. Mol. Med. Vol 16, No 6, 2012 pp. 1321-1330

Molecular mechanisms controlling *CFTR* gene expression in the airway

Zhaolin Zhang [a, b], Christopher J. Ott [a, b, §], Marzena A. Lewandowska [a, b, #], Shih-Hsing Leir [a, b], Ann Harris [a, b, *]

[a] *Human Molecular Genetic Program, Children's Memorial Research Center, Chicago, IL, USA*
[b] *Department of Pediatrics, Northwestern University Feinberg School of Medicine, Chicago, IL, USA*

Received: July 07, 2011; Accepted: August 05, 2011

Abstract

The low levels of *CFTR* gene expression and paucity of CFTR protein in human airway epithelial cells are not easily reconciled with the pivotal role of the lung in cystic fibrosis pathology. Previous data suggested that the regulatory mechanisms controlling *CFTR* gene expression might be different in airway epithelium in comparison to intestinal epithelium where CFTR mRNA and protein is much more abundant. Here we examine chromatin structure and modification across the *CFTR* locus in primary human tracheal (HTE) and bronchial (NHBE) epithelial cells and airway cell lines including 16HBE14o- and Calu3. We identify regions of open chromatin that appear selective for primary airway epithelial cells and show that several of these are enriched for a histone modification (H3K4me1) that is characteristic of enhancers. Consistent with these observations, three of these sites encompass elements that have cooperative enhancer function in reporter gene assays in 16HBE14o- cells. Finally, we use chromosome conformation capture (3C) to examine the three-dimensional structure of nearly 800 kb of chromosome 7 encompassing *CFTR* and observe long-range interactions between the *CFTR* promoter and regions far outside the locus in cell types that express high levels of CFTR.

Keywords: *CFTR* • gene expression • airway epithelium • DHS • histone modification • enhancer • 3C

Introduction

The recent development of new technologies to identify regulatory elements in non-coding regions of the human genome and elucidate their function [1] has enabled rapid advances in our understanding of many important genes. One such gene is the cystic fibrosis transmembrane conductance regulator (*CFTR*), which when mutated causes the common inherited disorder cystic fibrosis (CF). *CFTR* is a large gene encompassing 189 kb of genomic DNA [2] and showing complex cell-type specific and temporal regulation (reviewed in Ref. [3]). Of particular note is the very wide range of levels of *CFTR* expression in different cell types, with up to 1×10^4 more mRNA in pancreatic ducts and colon carcinoma cell lines than in primary cultures of tracheal and bronchial epithelium [4, 5]. Extensive characterization of the *CFTR* promoter region (reviewed in Ref. [3]) did not reveal elements that were responsible for cell-type-specific expression of the gene. Hence, we used several methods to find regions of open chromatin (DNase I hypersensitive sites, DHS) across the locus and in flanking sequences to find the critical *cis*-acting elements (reviewed in Ref. [3]). We identified enhancer-blocking insulator elements that flank the *CFTR* gene at −20.9 kb with respect to the translational start site and at +15.6 kb 3' to the translational stop site which likely establish the functional limits of the locus in at least some cell types. The −20.9 kb region binds CCCTC-binding factor (CTCF) [6], which is associated with many insulator elements, although the +15.6 kb element does not. However, additional DHS 3' to the locus coincide with CTCF and cohesin (Rad21) binding sites [5, 7]. DNase I hypersensitive sites within the first and eleventh introns encompass intestinal/genital duct restricted enhancer elements, which cooperate in reporter gene constructs to augment CFTR promoter activity about 40-fold. Our current model for the active *CFTR* locus presents a looped structure,

[§]Current address: Dana Farber Cancer Institute, Harvard Medical School, Boston, MA, USA.
[#]Current address: Molecular Oncology and Genetics Unit, The Lukaszczyk Oncology Center, Bydgoszcz, Poland.
*Correspondence to: Ann HARRIS,
Human Molecular Genetic Program, Children's Memorial Research Center, Chicago, IL 60614, USA.
Tel.: +1-773-755-6525
Fax: +1-773-755-6593
E-mail: ann-harris@northwestern.edu

doi:10.1111/j.1582-4934.2011.01439.x

which brings the insulators and distal *cis*-acting enhancer elements into close association with the promoter. These direct associations were measured by quantitative chromosome conformation capture (3C) [8]. However, when presenting this model we noted its relevance to *CFTR* expression in cell types that express abundant *CFTR*, such as primary epididymis epithelial cells and the intestinal cell lines Caco2 and HT29, but also suggested that the low levels of *CFTR* expression in primary airway epithelial cells might be mediated by different mechanisms [5]. In an effort to elucidate these, we now concentrate on the regulatory elements that may coordinate *CFTR* expression in airway epithelial cells. We identify cell-type-specific DHS that are seen in primary airway epithelial cells but not in airway cell lines that express much higher levels of *CFTR* mRNA such as 16HBE14o-. We also describe a novel DHS close to the *CFTR* promoter that is unique to this cell line. Next, we investigate epigenetic modifications at the *CFTR* locus and flanking regions in primary airway cells: enrichment of specific histone variants that are associated with enhancers (H3K4me1) and repressed chromatin (H3K27me3) [9] are evaluated. Several of the DHS are seen to encompass regions of H3K4me1 enrichment while H3K27me3 is evident immediately 5' to the gene promoter in primary airway cells, but not in other cell types that express *CFTR*. Elements within the DHS that are enriched for H3K4me1 are next shown to function as cell-type-specific enhancer elements that cooperate in reporter gene assays. Finally, we examine long-range interactions across nearly 800 kb flanking the *CFTR* locus to determine whether airway-specific DHS that are located distal to the enhancer blocking insulator elements at −20.9 kb and +15.6 kb are able to physically interact with the *CFTR* promoter, despite these barriers. These studies advance our understanding of the cell-type-specific regulation of *CFTR* and highlight mechanisms that may coordinate the low expression levels that are characteristic of primary airway cells.

Materials and methods

Cell culture

Primary skin fibroblasts (Coriell GM08333) were grown in minimal essential media (MEM; Invitrogen, Carlsbad, CA, USA) supplemented with 15% foetal bovine serum (FBS). Primary tracheal epithelial cells were extracted from post-mortem human adult trachea as previously described with minor modifications [10]. NHBE cells, a mixture of primary human bronchial and tracheal epithelial cells (CC-2541; Lonza, Walkersville, MD, USA) were cultured in BEGM (Lonza) per the manufacturer's instructions. Transformed human bronchial epithelial cell lines 16HBE14o- [11] and Beas2B [12] and the lung carcinoma cell line Calu3 [13] were grown in DMEM with 10% serum. All cells were grown on plastic at liquid interface.

Primer sequences

All primer sequences and locations used for DNase-chip, RT-PCR, plasmid cloning and mutagenesis and 3C are listed in the Supporting information.

DNase-chip

DNase-chip was performed as previously described, with modifications [14]. Briefly, 2–5 × 10^7 cells were lysed using 0.1% NP-40 buffer. Purified nuclei were exposed to increasing amounts of DNase I (0–30 U; NEB, Ipswich, MA, USA), reactions were stopped with 0.1M EDTA, and digested chromatin was embedded into InCert agarose plugs (Lonza). Chromatin digestion was determined by pulsed field gel electrophoresis and adequately digested samples were blunt-ended with T4 DNA polymerase (NEB). Chromatin was then extracted from agarose, and blunt ends were ligated to biotinylated linkers overnight. As a control, 25 μg of genomic DNA from the same cell type was ligated to linkers and processed in parallel. Chromatin was sonicated to generate 200–500 bp fragments, and biotinylated ends were captured with steptavidin Dynabeads (Invitrogen). Sheared ends were blunted with T4 DNA polymerase and ligated to non-biotinylated linkers, and samples were amplified with ligation-mediated PCR using primer oJW102C. PCR material was labelled with Cy5-dUTP and genomic DNA control labelled with Cy3-dUTP, and each hybridized to ENCODE tiling arrays (NimbleGen, human genome build 17, May 2004). Hybridization data from three (Caco2 and fibroblasts) or two (16HBE14o-) experiment was analysed with ACME statistical software [15] using a window size of 500 bp and a threshold of 0.95.

Chromatin immunoprecipitation

Primary cells were cross-linked directly on the cell culture plates, long-term cell lines were trypsinized, resuspended in DMEM and cross-linked with 0.37% formaldehyde for 10 min. Cross-linking was stopped by the addition of glycine to 0.125M. Cells were washed with cold PBS and for 1 × 10^7 cells lysed in 1 ml of 1% SDS, 10 mM EDTA, 50 mM Tris/HCl pH 8.1, 1× protease inhibitor cocktail (Roche, Indianapolis, IN, USA). Chromatin was sonicated to an average size of 200–500 bp.

Immunoprecipitations were performed overnight at 4°C using 100 μl chromatin that was diluted 1:10 with ChIP dilution buffer (0.01% SDS, 1.1% Triton X-100, 1.2 mM EDTA, 16.7 mM Tris-HCl pH 8.1, 167 mM NaCl), 4 μg BSA and 10 μg of antibodies specific for H3K27me3 (07-499; Millipore, Billerica, MA, USA), H3K4me1 (07-436; Millipore) or rabbit IgG (sc-2027; Santa Cruz, Santa Cruz, CA, USA). Complexes were collected using 60 μl Protein A/Salmon sperm agarose beads (16-157; Millipore), washed several times according to the manufacturers protocol and eluted with 1% SDS, 0.1M $NaHCO_3$. Crosslinks were reversed at 65°C for 4 hrs, and samples were treated with RNase (10 μg/ml) and Proteinase K (40 μg/ml) before phenol/chloroform extraction and ethanol precipitation. Samples were resuspended in 0.5× TE and enrichment was analysed using SYBR Green qPCR. PCR primers are listed in Table S1.

Transient promoter/enhancer reporter assays

Sequences encompassing the DHS at –35 kb (hg 17, chr7:116,678,400-116,680,000), −3.4 kb (hg17, chr7:116,710,076–116,711,290) and in intron 23 at 4374 + 1.3 kb (hg17, chr7:116,899,700-116,901,100) were amplified by PCR using Pfu DNA polymerase (Stratagene). Primers are shown in Table S1. Reporter assays were performed by standard methods using a reporter gene construct driven by the 787 bp CFTR minimal promoter (pGL3B 245) [16, 17].

Chromosome conformation capture (3C)

3C was performed as described previously [8, 7], with minor modifications. Briefly, 1 × 10^7 cells were fixed with 2% formaldehyde for 10 min. at room

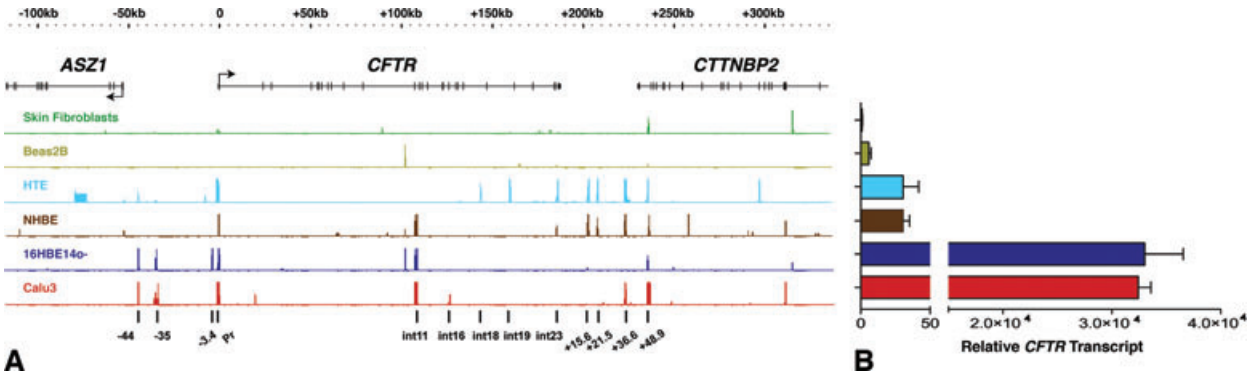

Fig. 1 Identification of DHS across the *CFTR* locus region in primary airway cells and airway cell lines. (**A**) Averaged DNase-chip hybridization data from at least two experiments on HTE, NHBE, 16HBE14o-, Calu3 and skin fibroblasts and one culture of Beas2B, were analysed with ACME statistical software [15]. The location of *ASZ1*, *CFTR* and *CTTNBP2* are shown at the top of the figure where the zero point of the *x*-axis represents the beginning of the first *CFTR* exon. A major DHS was identified at the *CFTR* promoter (Pr) in all cells that express the gene and other cell-selective DHS of interest are marked below the hybridization tracks. The *y*-axis for each DHS track represents-log 10 (*P*-value) between 0 and 16 as determined by ACME. (**B**) *CFTR* mRNA levels measured by qRT-PCR; each value is relative to the transcript level in skin fibroblasts. Error bars represent S.E.M., $n = 3$.

temperature. Cells were lysed in 5 ml cold lysis buffer [10 mM Tris (pH 8), 10 mM NaCl, 0.2% NP-40, 1× protease inhibitor cocktail (Roche)] and the nuclei collected by centrifugation. Following extraction with 0.3% SDS, chromatin was digested overnight with 2000 U *Hind* III. Ligations were performed in a total reaction volume of 6.5 ml, using 100 U T4 DNA ligase (Roche) and incubation at 14°C for 4 hrs followed by 30 min. at room temperature. Cross-links were reversed by proteinase K treatment at 65°C overnight. Samples were purified by phenol–chloroform extraction followed by ethanol precipitation, and then resuspended in 150 μl H_2O. The concentration of each sample was determined by SYBR green qPCR, using the B13F/B13R primer set (amplicon found within a *Hind* III fragment; see Supporting Information) and comparison to a genomic DNA reference of known concentration. Samples were subsequently diluted to a concentration of 100 ng/μl. A Taqman probe and reverse primer were designed that were specific to a *Hind* III fragment at the *CFTR* promoter (bait). Multiple forward primers were then designed that were each specific to different *Hind* III fragments across the *CFTR* locus (see Table S1 for primer and probe sequences and locations). Using a dilution series of digested/religated BAC DNA template, each forward primer was demonstrated to function with the 'fixed' Taqman probe and reverse primer to amplify with 100% efficiency. To quantify ligation events within 3C samples, 200 ng of 3C template was used per 20 μl Taqman qPCR reaction. The ligation efficiency (or 'interaction frequency') between each fragment and the *CFTR* promoter was corrected for the interaction between two *Hind* III fragments within the ubiquitously expressed Excision repair cross-complementing rodent repair deficiency, complementation group 3 (*ERCC3*) locus, which has been reported to adopt the same spatial conformation in different tissues [18].

Results

Detection of novel DHS at the *CFTR* locus in airway epithelial cells

We previously evaluated DHS across the *CFTR* locus by DNase chip in intestinal cell lines, primary male genital duct epithelial cells and primary tracheal and bronchial epithelial cells and identified both cell-type-specific and ubiquitous DHS. Here we focus on primary human tracheal and bronchial epithelial cells and compare these to airway epithelial cell lines that are frequently used in CF research. Figure 1A shows DNase chip data for skin fibroblasts that do not express *CFTR*, Beas2B cells that express almost undetectable levels, primary human tracheal epithelial (HTE) cells and a mixture of human bronchial and tracheal epithelial cells (NHBE), which express low levels of *CFTR*, 16HBE14o- and Calu3 cells that express very high levels of *CFTR*, which are comparable to those seen in intestinal cell lines. Relative levels of the *CFTR* transcript in each line are shown in Figure 1B. (These do not necessarily correlate with the levels of functional CFTR protein in each line.)

The first notable feature of the DNase chip data in Figure 1A is the presence of several DHS at the 3' end of the *CFTR* locus and between *CFTR* and *CTTNBP2* in the primary HTE and NHBE cells that are absent from the airway cell lines, despite the much higher levels of *CFTR* transcript in the latter (Fig. 1B). Also of note are several DHS that are apparently unique to HTE cells. All cell types that express *CFTR* show a DHS at the promoter as expected and NHBE, 16HBE14o- and Calu3 cells also show a DHS in intron 11 that we identified in intestinal cells [5]. Beas2B, NHBE and 16HBE14o− cells exhibit a DHS in intron 10 (10c, Refs. [19, 20]) that was seen in many cells types irrespective of *CFTR* expression. Of particular interest are DHS seen at −44 kb and −35 kb from the translational start site in HTE, 16HBE14o- and Calu3 cells and at +36.6 kb 3' to the last exon in HTE, NHBE and Calu3 cells. The DHS at +48.9 kb from the 3' end of the *CFTR* gene, which is located in the last intron of the neighbouring *CTTNBP2* locus and is seen in all the cell types analysed here, corresponds to a ubiquitous CTCF binding site that binds the cohesin complex subunit Rad21 [5]. Novel DHS were seen in Calu3 cells, in intron 1 (at 185 + 20 kb) and intron 16 (at 3120 + 1 kb), which have not been detected in any other cell type that we have examined. However, we previously identified a region of strong cross-species homology encompassing the 3120 + 1 kb DHS and evaluated

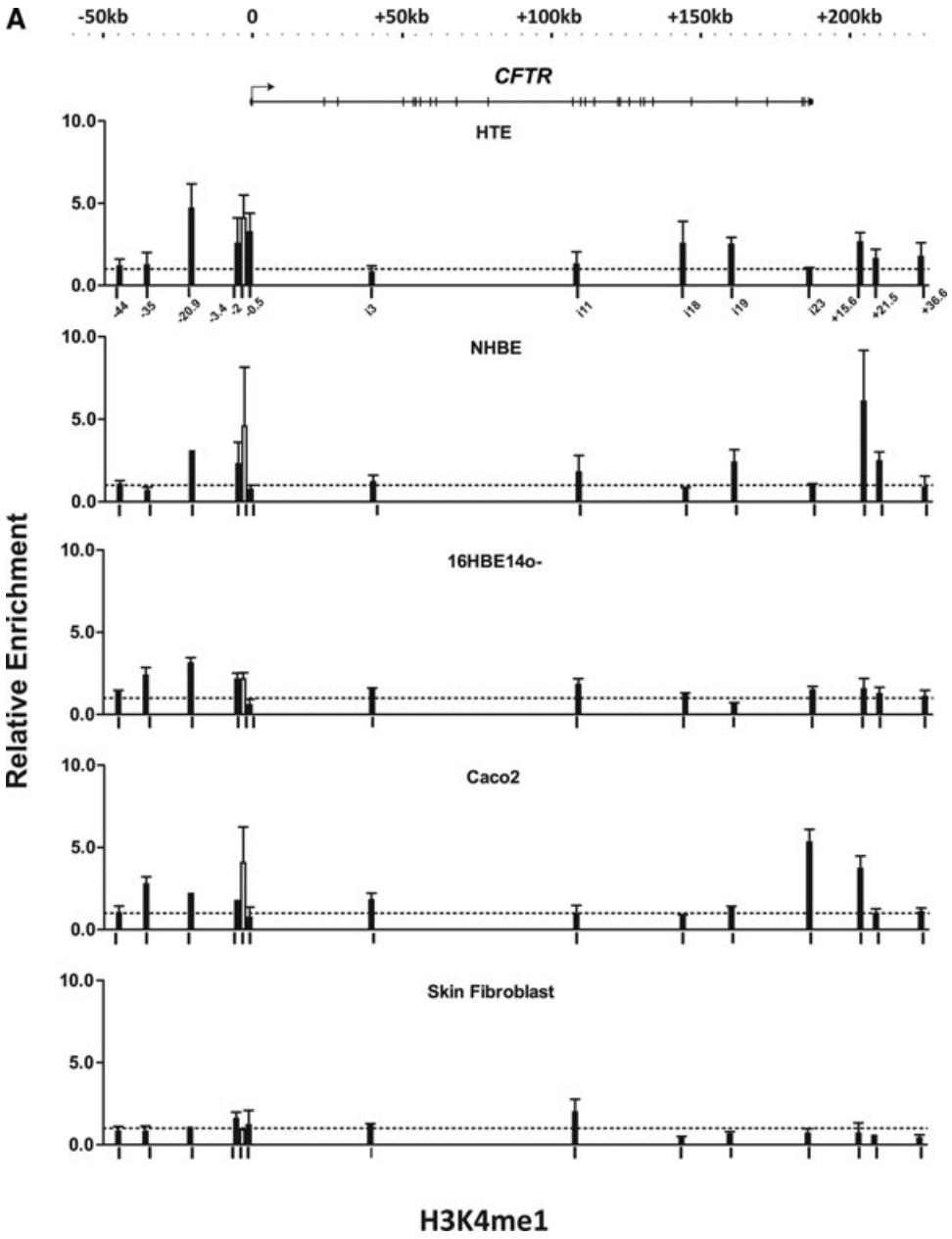

Fig. 2 Histone modifications across the *CFTR* locus region in airway epithelial cells. Real-time PCR analysis of chromatin from HTE, NHBE, 16HBE14o-, Caco2 and skin fibroblasts, immunoprecipitated with antibodies specific to (**A**) H3K4me1 and (**B**) H3K27me3. Primer sets (Table S1) are at multiple sites along the locus, shown by locators on the *x*-axis of the top graph. Black bars below each graph mark equivalent sites. Each value shown is relative to enrichment measured with isotype-matched IgG control (dotted line). Data for each cell line are combined from at least two ChIP experiments. All data points were calculated as percentage of input material and then normalized to background 18s rRNA levels; error bars represent S.E.M. of at least two PCR reactions in biological replicas for each fragment. The *CFTR* locus is shown at the top of the figure.

DNA–protein interactions *in vitro*, in the absence of a functional element [21]. Also of interest were DHS that were only detected in the primary HTE and NHBE airway epithelial cells in introns 18 (chr7:116,858,000–116,858,500), 19 (chr7:116,873,900–116,874,800) and 23 (chr7:116,899,700–116,901,100). In an initial effort to reveal the functions of the elements located within these DHS, we first sought to determine epigenetic signatures at these sites. Because we previously characterized cell-type (intestinal) specific intronic enhancers in introns 1 and 11 of *CFTR*, we evaluated each of these novel airway DHS for a histone modification that is associated with enhancer elements and another associated with repressed chromatin.

Histone modifications across the *CFTR* locus in airway epithelial cells predict enhancers located within several DHS sequences

Chromatin immunoprecipitation was carried out on skin fibroblasts (a negative control for *CFTR* expression), primary HTE and NHBE cells, 16HBE14o− and Caco2 cells (a colon carcinoma cell line with very high *CFTR* expression levels, similar to those seen in 16HBE14o−), with antibodies specific for modifications seen at enhancers (H3K4me1; Fig. 2A) and in repressed chromatin (H3K27me3; Fig. 2B). More recently, the H3K27me3 mark was also

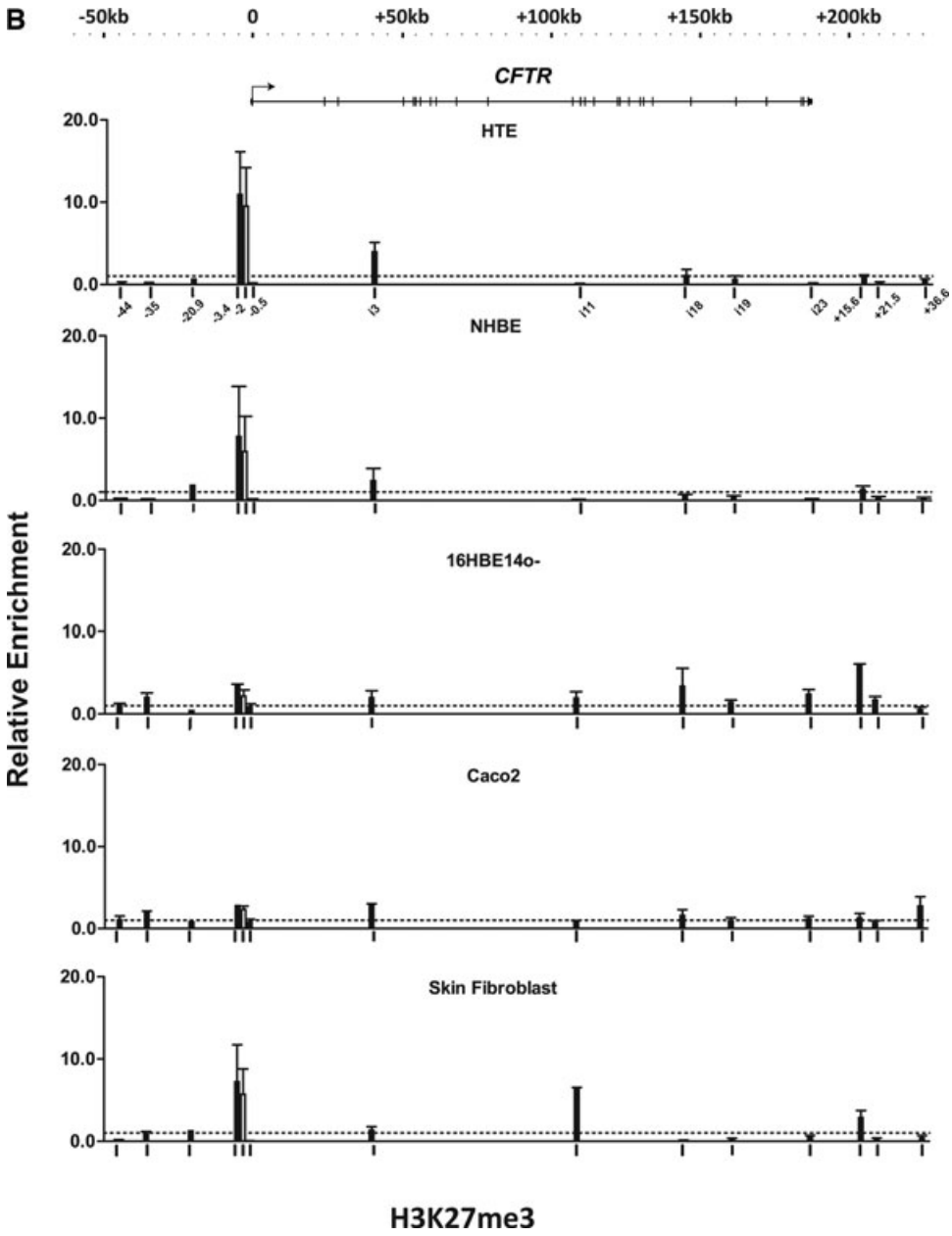

Fig. 2 Continued.

shown to be enriched at poised developmental enhancers [22]. Primer sets for the SYBR green qPCR were designed to amplify regions within the DHS identified in the airway cell types together with other tissue-specific or ubiquitous DHS reported previously [5] (primer sequences are shown in Table S1). H3K4me1 was primarily evident at the *CFTR* promoter in the primary tracheal epithelial (HTE) cells with greatest enrichment at −2 kb and lesser enrichment at −3.4 kb and −0.5 kb with respect to the translational start site. The ChIP profile of NHBE cells at the promoter was very similar to that of Caco2 colon carcinoma cells, with highest enrichment at −2 kb and no enrichment at −0.5 kb. However, 16HBE14o− bronchial epithelial cells showed little H3K4me1 in the promoter region. Additional minor peaks of H3K4me1 were seen at the −35 kb DHS in both 16HBE14o- and Caco2 and intron 23, at 4374 + 1.3 kb, primarily in Caco2 (with only very minor enrichment in 16HBE14o−). The enhancer-blocking insulator element at +15.6 kb [6] shows H3K4me1 enrichment in multiple cell types, most notably HTE, NHBE and Caco2. Also of interest were minor peaks of H3K4me1 at DHS in introns 18, 19 and at +36.6 kb, which were most evident in primary tracheal epithelial cells.

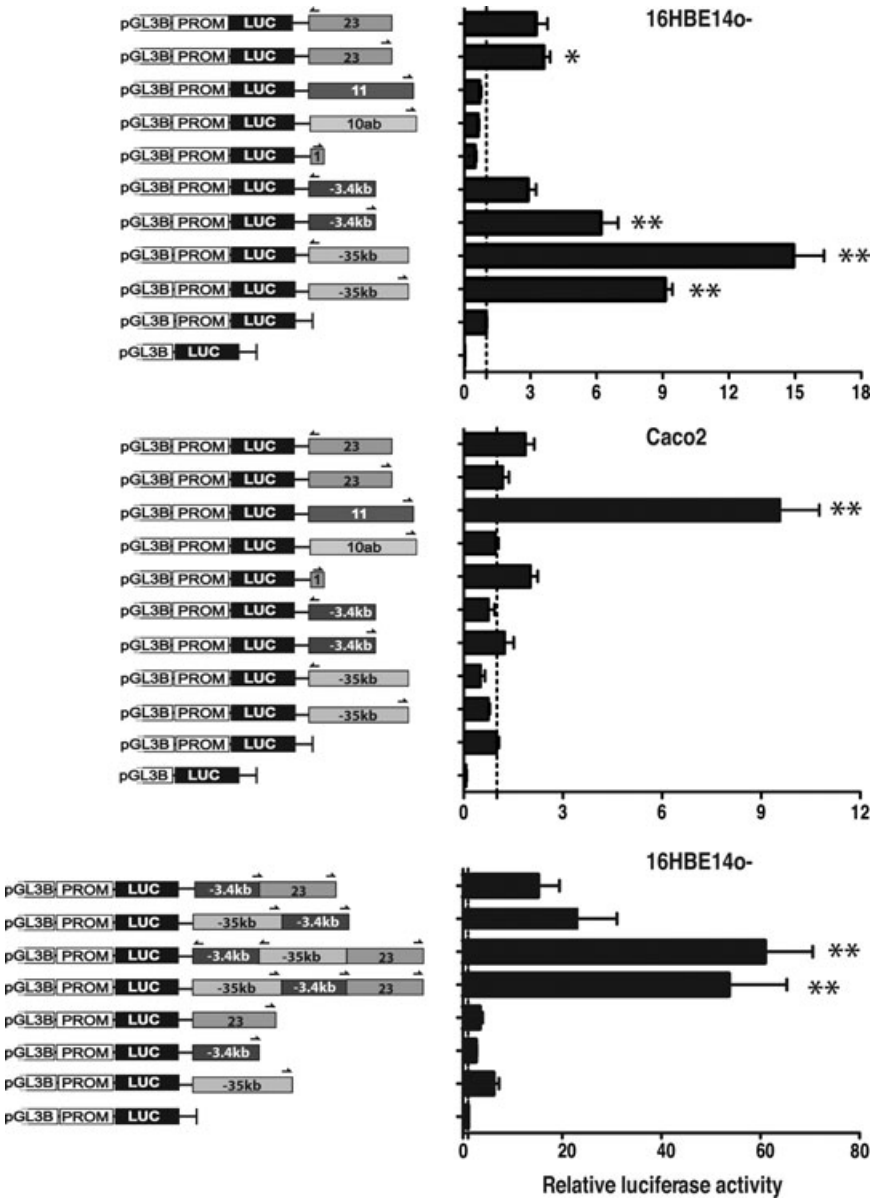

Fig. 3 −35 kb, −3.4 kb and intron 23 DHS encompass enhancer elements that activate the *CFTR* basal promoter and cooperate with each other. (**A**) 16HBE14o− and (**B**) Caco2 cells were transfected with pGL3B luciferase reporter constructs containing the 787 bp *CFTR* basal promoter (pGL3B 245) and fragments of the DHS regions at −35 kb, −3.4 kb and intron 23 cloned into enhancer site of the vector in either forward or reverse orientations. Control transfections included known intestinal enhancers (active in Caco2) in introns 1 and 11 and a non-enhancer sequence, intron 10a,b. (**C**) 16HBE14o− cells transfected with the same pGL3B 245 construct and multiple combined elements within the enhancer site as shown. Data are shown in (**A**) and (**B**) relative to the *CFTR* basal promoter-alone vector and in (**C**) to the single element enhancer constructs; error bars represent S.E.M. ($n = 6$), $^{*}P < 0.01$ and $^{**}P < 0.001$ using unpaired *t*-tests.

H3K27me3 ChIP showed generally very low levels of this modification at the airway-specific DHS with minor enrichment at several elements, including in intron 18 and +15.6 kb in 16HBE14o− cells. Of particular note in primary HTE and NHBE cells, H3K27me3 was abundant at the −3.4 kb and −2 kb promoter regions but not the −0.5 kb region. Fibroblasts, which lack *CFTR* expression showed H3K27me3 enrichment across all three sites evaluated within the promoter region and at the intron 11 region that is associated with enhancer function in intestinal and genital duct cells that express high levels of CFTR.

The −35 kb, −3.4 kb and intron 23 (4374 + 1.3 kb) DHS contain cell-type-specific enhancers

To test our prediction that the DHS regions that were enriched for H3K4me1 encompassed enhancer elements, three DHS at −35 kb, −3.4 kb and in intron 23 (4374 + 1.3 kb), were chosen for further study. Each region was amplified and cloned (in both orientations) into the enhancer site of the pGL3B 245 vector [16] in which luciferase reporter expression is driven by a 787 bp *CFTR* basal promoter fragment. These constructs were co-transfected with a

renilla control plasmid into 16HBE14o- (Fig. 3A) and Caco2 cells (Fig. 3B) and relative luciferase expression measured. Additional constructs used in these assays were described previously [5] and contained DHS elements from intron 1 (185 +10 kb), intron 10 (1716 + 13.2/13.7 kb) and intron 11 (1811 + 0.8 kb) of *CFTR* in the enhancer site of the vector. The introns 1 and 11 constructs contain intestinal-specific enhancers that are active in Caco2 cells but not in 16HBE14o- cells [16, 23, 24, 5], while the intron 10a,b, elements do not encompass an enhancer [17, 5]. In 16HBE14o- bronchial epithelial cells, the fragment encompassing the −35 kb DHS acted as a strong enhancer that significantly increased CFTR promoter activity 9- and 15-fold in forward and reverse orientations, respectively. The elements spanning the DHS at −3.4 kb and within intron 23 (4374 + 1.3 kb) had more modest enhancer activity, with three-fold effect on the *CFTR* promoter in reverse orientation for −3.4 kb and both orientations for intron 23 and six-fold effect for −3.4 kb in the forward orientation. Two copies of the −3.4 kb element approximately doubled the enhancer activity of this element (data not shown). The −35 kb and −3.4 kb DHS regions had no enhancer activity in Caco2 cells, although the intron 23 element had a slight effect, increasing the promoter activity by 1.8-fold (Fig. 3B), which was not statistically significant. These data are consistent with the absence of the −35 kb and −3.4 kb DHS from the Caco2 cells, with a very minor DHS in intron 23 [5]. The data also suggest that DHS at −35 kb and −3.4 kb contain airway-selective enhancers while the intron 23 (4374 + 1.3 kb) DHS encompasses an enhancer that may function in airway and intestinal epithelial cells, but is more effective in the airway.

Because we previously showed that the intestinal-specific enhancer elements within intron 1 and intron 11 function cooperatively when cloned together into the enhancer site of the pGL3 245 vector, we next generated constructs in which the −35 kb, −3.4kb and intron 23 elements were cloned into pGL3B 245 together with the intron 11 enhancer region. However, we saw no evidence of cooperation between these elements in either 16HBE14o- or Caco2 cells (data not shown). In contrast, when we combined the −35 kb, −3.4 kb and intron 23 elements together in the enhancer site of the pGL3 245 vector they showed cooperative interactions, with a 60-fold increase in enhancer activity in comparison to the promoter alone. The −35 kb and intron 23 elements combined independently in pairs with the −3.4 kb element also showed cooperative activity though the values were threefold lower than the three elements combined.

Longer range interactions across 800 kb spanning the *CFTR* locus

Because we observed cell-type-specific DHS in airway epithelial cells at −44 kb, −35 kb, +21.5 kb and 36.6 kb DHS, which were distal to the enhancer blocking insulators characterized at −20.9 and +15.6 kb with respect to the *CFTR* gene, we next used chromosome conformation capture (3C, Ref. [8]) to investigate whether these sites associated with the *CFTR* promoter by a looping mechanism. We also evaluated the expression of the flanking genes *ASZ1* and *CTTNBP2* in these cell types to determine whether the more distal DHS could be involved in the regulation of these loci. Semi-quantitative RT-PCR and microarray analysis demonstrated that *ASZ1* was not expressed in NHBE, HTE and 16HBE14o- cells, although trace amounts were detected in Caco2 (data not shown). Thus, the 5' DHS are more likely to be associated with regulatory elements for *CFTR* than *ASZ1*. In contrast, *CTTNBP2* transcripts were evident in variable amounts in NHBE, HTE and Caco2 cells but were not detected in 16HBE14o-. Thus, we cannot exclude the possibility that the DHS 3' to *CFTR* contain regulatory elements that influence *CTTNBP2* expression instead of, or in addition to *CFTR*.

For the 3C experiments, we used a 'bait' Taqman probe and reverse primer located at the *CFTR* promoter (described previously, Ref. [7]) and forward primers close to the 3' end of *Hind* III fragments spanning from hg 17, chr7:116,387,846–117,180,423, a genomic distance of 790,420 kb. Real-time PCR reactions using the probe/reverse primer and each of the forward primers enabled quantification of ligation events (subsequently referred to as 'interaction frequency') between the *CFTR* promoter and specific distal regions within each sample. Hence, the forward primers in *Hind* III fragments enabled us to measure directly whether elements within these regions were physically associated with the *CFTR* promoter region. Figure 4 shows that, although no long-distance interactions are evident in skin fibroblasts, where the *CFTR* promoter is inactive, in NHBE cells there is a very slightly elevated interaction of the promoter with the −35 kb DHS and a fragment located at +20 kb with respect to the end of the transcript, although these are likely not significant. In contrast, 5' to the locus in 16HBE14o− cells, although no interaction is event with the −35 kb DHS region, the −79.5 kb DHS [25] and a *Hind* III fragment encompassing −163 kb showed higher interaction frequencies with the *CFTR* promoter. 3' to the locus, strong interactions with the promoter were seen at +20 kb and to a lesser extent at +109 kb. A similar pattern of distal interactions was seen in Caco2 cells that we showed previously to demonstrate strong looping of intragenic and more proximal flanking regions of the *CFTR* locus [5]. Thus, despite the presence of enhancer blocking insulators at −20.9 and +15.6 kb 5' and 3', respectively, to the *CFTR* gene, a higher order of chromatin interactions is seen in cell types that express high transcript levels, which brings more distal (>100 kb away from the locus) genomic regions into close association with the active *CFTR* promoter.

Discussion

Variation in the utilization of *cis*-acting regulatory elements is not uncommon as a mechanism for achieving cell-type-specific regulation of gene expression. Here we identify novel *cis*-acting elements associated with DHS in the active *CFTR* gene in primary airway epithelial cells (HTE and NHBE) or airway epithelial cell lines (16HBE14o-, Calu3 and Beas2B). These sites were not evident in

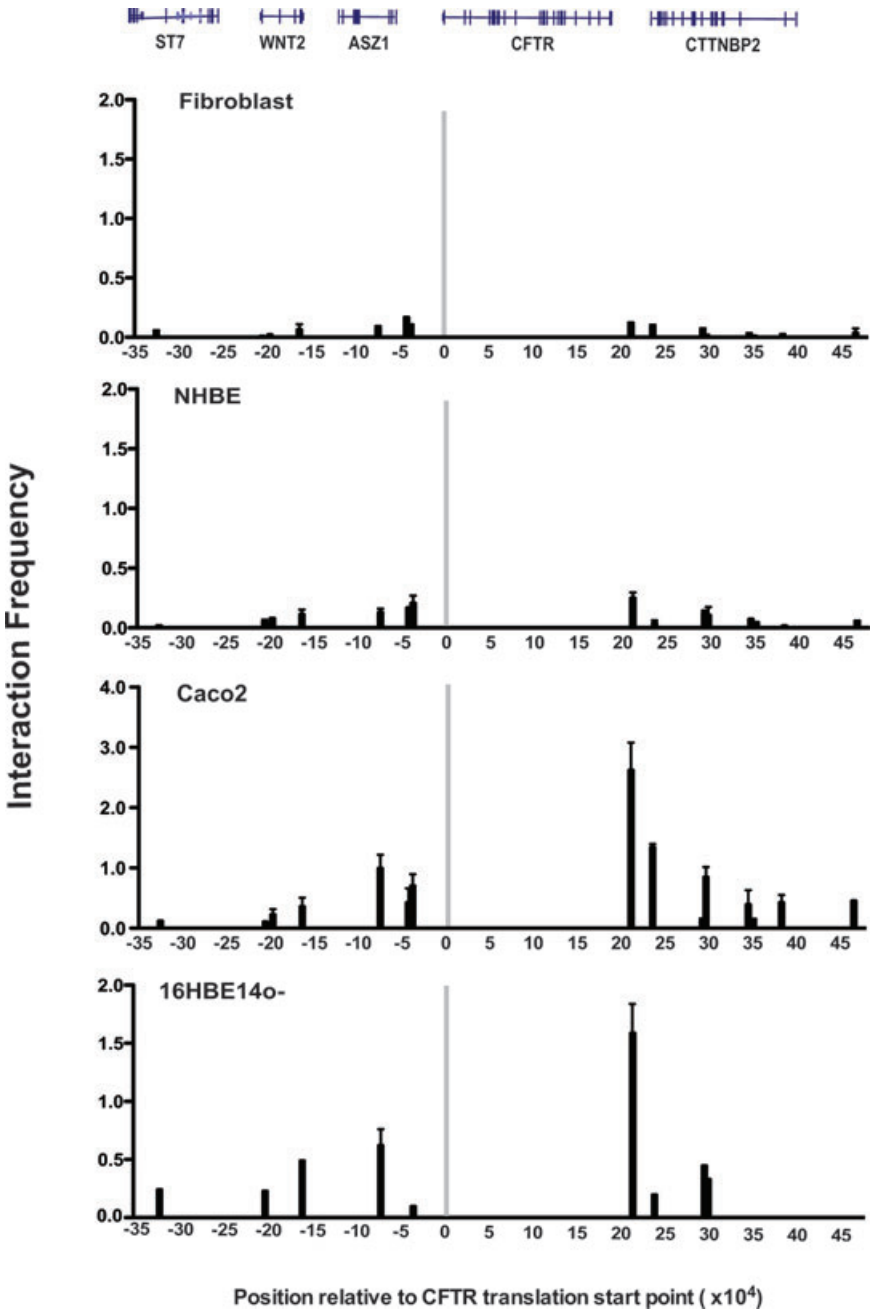

Fig. 4 Long-range interactions between the *CFTR* promoter and specific DHS measured with q3C. The organization of the *ASZ1, CFTR* and *CTTNBP2* loci are displayed above the graphs. The grey bar represents the 'bait' region of the *CFTR* promoter, which includes a primer and Taqman probe adjacent to the 5' *Hind* III site; this *Hind* III fragment spans the identified *CFTR* transcriptional start sites. The *x*-axis in each graph represents the location of the 3' end of each assayed *Hind* III fragment relative to the translational start site; the *y*-axis represents interaction frequency relative to the interaction frequency between two *Hind* III fragments within the ubiquitously expressed *ERCC3* gene. Data for each cell type are from a single representative 3C experiment (each experiment performed at least twice in duplicate), error bars represent S.E.M. of at least two PCR reactions for each fragment.

colon carcinoma cell lines such as Caco2 that express very high levels of *CFTR*, more than 10,000-fold more than is seen in primary tracheal and bronchial epithelial cells (when estimated by qRT-PCR). However, these different DHS profiles cannot be accounted for solely by mechanisms that coordinate expression of high levels of *CFTR* because the bronchial epithelial cell lines 16HBE14o- and Calu3 both express abundant *CFTR*, equivalent to that seen in Caco2 cells, but lack the DHS seen in primary airway epithelial cells. Of particular interest are DHS at −44 kb, −35 kb with respect to the translational start site and in introns 18 (chr7: 116,858,000–116,858,500), 19 (chr7:116,873,900–116,874,800) and 23 (chr7:116,899,700–116,901,100) that are evident in primary HTE and NHBE cells. The −44 kb and −35 kb DHS are also evident in 16HBE14o− and Calu3 cells. Also of interest was the DHS at −3.4 kb, which was distinct from the major promoter DHS in 16HBE14o− cells.

The enrichment of H3K4me1 within DHS at −35 kb, −3.4 kb and intron 23 (4374 + 1.3 kb) predicted that these sites might encompass enhancer elements, despite the fact that the −35 kb and intron 23 sites are evident in the primary airway cells, which show very low levels of *CFTR* expression. All three elements showed enhancer activity when cloned into a pGL3 vector, in which luciferase expression is driven by the *CFTR* basal promoter, and transfected into 16HBE14o- cells. The −35 kb site showed the most robust enhancer activity, with about 15-fold increase over the basal promoter alone in 16HBE14o- cells, and the element is inactive in Caco2 colon carcinoma cells, consistent with absence of the DHS from this line. For comparison it is notable that the intron 11 strong intestinal enhancer, which we described previously [5], augments CFTR promoter activity in Caco2 cells at a level comparable to that of the −35 kb enhancer in 16HBE14o- cells (Fig. 3B), but lacks activity in 16HBE14o- cells. Together, these data demonstrate the cell-type selectivity of each site. The intron 23 element has modest enhancer activity in comparison and this is evident in 16HBE14o− cells but is not significant in Caco2 cells, which show a very minor DHS at this site [5]. The −3.4 kb DHS is of additional interest since it has moderate enhancer activity in 16HBE14o- cells but not in Caco2 where the DHS is not evident. However, this activity is orientation-dependent in the enhancer site of pGL3B only showing significance when the element is cloned in the forward orientation. Thus, it is not behaving as a classical enhancer and may encompass another type of regulatory element. Also of interest is the observation that the −35 kb, −3.4 kb and intron 23 elements cooperate when inserted together into the enhancer site of the pGL3B 245 construct. However, these elements do not cooperate with the intestinal-specific DHS in introns 1 and 11, which we showed previously to cooperate with each other in intestinal cells. This further supports our suggestion that different regulatory mechanisms control *CFTR* expression in the airway and the intestinal epithelium.

The question arises as to how the primary airway cells (HTE and NHBE) maintain *CFTR* expression at very low levels, when they exhibit DHS that encompass strong enhancer elements. A trivial explanation would be that although expression levels are very low in the airway cell cultures as a whole, small numbers of cells may achieve high levels of transcription by recruitment of these enhancer elements. Alternatively, a partial explanation may be provided by our ChIP data on the repressive chromatin mark H3K27me3, which is abundant at the −3.4 kb and −2 kb promoter regions but not the −0.5 kb region in these cells. In fibroblasts, where the *CFTR* locus is inactive, H3K27me3 enrichment is seen at all three sites evaluated within the promoter region but in contrast, there is no evidence for this histone modification in cells with a highly active *CFTR* locus, such as 16HBE14o− and Caco2. The significance of the H3K27me3 mark at promoter regions in the context of models of repressive transcription has been discussed elsewhere [22]. It is possible that there is a competition occurring at the *CFTR* promoter between Trithorax group (TrxG) activating proteins and Polycomb group (PcG) repressive proteins including polycomb repressive complexes 1 and 2 (PRC1 and PRC2). The latter protein generates the H3K27me3 mark, which can spread across chromatin domains. In contrast, TrxG proteins catalyse a different histone modification (H3K4me3) that activates transcription. Possibly fine control of this competition at the *CFTR* promoter can regulate low levels of expression (high H3K27me3 at the −3.4 and −2 kb DHS, but not at −0.5 kb), turn off promoter activity completely (high H3K27me3 spreading from the −2 kb site to the −0.5 kb site), or enable high levels of promoter activity where PRC2 is totally replaced by TrxG proteins and there is no evidence of H3K27me3.

Another question that arises from our data is how regulatory elements that lie distal to the enhancer blocking insulators that flank the *CFTR* locus can influence promoter activity. We previously identified and characterized a 5' insulator associated with a DHS at −20.9 kb to the gene, which binds CTCF and another +15.6 kb 3' to the locus which does not [6]. The −20.9 kb site is not evident on the DNase chip data shown in Figure 1A due to the presence of adjacent repetitive elements which are excluded from the microarray. However, we showed the site was present in multiple cell types [25, 26] and it is seen on DNase seq analysis of both HTE and NHBE cells (unpublished data). However, despite the presence of these enhancer blocking insulators, the long range 3C data shown in Figure 4 suggest that at least in airway cell types that express high levels of *CFTR* such as 16HBE14o-, chromosome looping enables regions that are up to ~100 kb 5' and 3' to the locus to be brought into close association with the gene promoter. These data are consistent with observations on HeLa and Caco2 cells [27] that demonstrated interaction of regions −80 kb 5' with the *CFTR* promoter. Moreover, they provide an explanation for the mechanism of action of the −35 kb enhancer element identified here in airway-specific regulation of *CFTR* expression, and demonstrate how it bypasses the −20.9 kb insulator element to interact with the promoter. Perhaps the classical enhancer-blocking assay [28] that we used to define the function of the *CFTR* insulators measures a function that is not active over these extremely long genomic distances *in vivo*.

In conclusion, we identified a novel set of cooperating enhancer elements that are associated with DHS within and flanking the *CFTR* gene in primary human tracheal and bronchial epithelial cells and are not found in many other cell types that express *CFTR*. We showed that though these sites may lie outside the insulator elements that flank *CFTR* they can still interact directly with the *CFTR* promoter by chromatin looping. Moreover, we showed that *CFTR* in primary airway epithelial cells appears to be regulated by different mechanisms from those seen in airway cell lines which have more than 10,000 times as much *CFTR* transcript. We suggest a mechanism involving local histone modifications at the *CFTR* promoter that may cause partial transcriptional repression in these primary airway cells, thus maintaining transcripts in low abundance. Future work will identify cell-type-specific *trans*-acting factors that mediate the function of these airway-specific elements.

Acknowledgements

We thank Dr Calvin Cotton for the primary HTE cultures, Dr Neil Blackledge for preparing the 3C libraries, and Dr Fabricio Costa for critical reading of the manuscript. This work was funded by a National Institutes of Health Grant R01 HL094585 (to A.H.)

Conflict of interest

The authors confirm that there are no conflicts of interest.

Supporting information

Additional Supporting Information may be found in the online version of this article:

Table S1. Primer sequences

Please note: Wiley-Blackwell is not responsible for the content or functionality of any supporting information supplied by the authors. Any queries (other than missing material) should be directed to the corresponding author for the article.

References

1. **Birney E, Stamatoyannopoulos JA, Dutta A, *et al.*** Identification and analysis of functional elements in 1% of the human genome by the ENCODE pilot project. *Nature.* 2007; 447: 799–816.
2. **Rommens JM, Iannuzzi MC, Kerem B, *et al.*** Identification of the cystic fibrosis gene: chromosome walking and jumping. *Science.* 1989; 245: 1059–65.
3. **Ott CJ, Harris A.** Genomic approaches for the discovery of CFTR regulatory elements. *Transcr.* 2011; 2: 23–7.
4. **Riordan JR, Rommens JM, Kerem B, *et al.*** Identification of the cystic fibrosis gene: cloning and characterization of complementary DNA. *Science.* 1989; 245: 1066–73.
5. **Ott CJ, Blackledge NP, Kerschner JL, *et al.*** Intronic enhancers coordinate epithelial-specific looping of the active CFTR locus. *Proc Natl Acad Sci USA.* 2009; 106: 19934–9.
6. **Blackledge NP, Carter EJ, Evans JR, *et al.*** CTCF mediates insulator function at the CFTR locus. *Biochem J.* 2007; 408: 267–75.
7. **Blackledge NP, Ott CJ, Gillen AE, *et al.*** An insulator element 3' to the CFTR gene binds CTCF and reveals an active chromatin hub in primary cells. *Nucleic Acids Res.* 2009; 37: 1086–94
8. **Hagege H, Klous P, Braem C, *et al.*** Quantitative analysis of chromosome conformation capture assays (3C-qPCR). *Nat Protoc.* 2007; 2: 1722–33.
9. **Zhou VW, Goren A, Bernstein BE.** Charting histone modifications and the functional organization of mammalian genomes. *Nat Rev Genet.* 2011; 12: 7–18.
10. **Davis PB, Silski CL, Kercsmar CM, *et al.*** Beta-adrenergic receptors on human tracheal epithelial cells in primary culture. *Am J Physiol.* 1990; 258: C71–6.
11. **Cozens AL, Yezzi MJ, Kunzelmann K, *et al.*** CFTR expression and chloride secretion in polarized immortal human bronchial epithelial cells. *Am J Respir Cell Mol Biol.* 1994; 10: 38–47.
12. **Reddel RR, Ke Y, Gerwin BI, *et al.*** Transformation of human bronchial epithelial cells by infection with SV40 or adenovirus-12 SV40 hybrid virus, or transfection *via* strontium phosphate coprecipitation with a plasmid containing SV40 early region genes. *Cancer Res.* 1988; 48: 1904–9.
13. **Fogh J, Wright WC, Loveless JD.** Absence of HeLa cell contamination in 169 cell lines derived from human tumours. *J Natl Cancer Inst.* 1977; 58: 209–14.
14. **Crawford GE, Davis S, Scacheri PC, *et al.*** DNase-chip: a high-resolution method to identify DNase I hypersensitive sites using tiled microarrays. *Nat Methods.* 2006; 3: 503–9.
15. **Scacheri PC, Crawford GE, Davis S.** Statistics for ChIP-chip and DNase hypersensitivity experiments on NimbleGen arrays. *Methods Enzymol.* 2006; 411: 270–82.
16. **Smith AN, Barth ML, McDowell TL, *et al.*** A regulatory element in intron 1 of the cystic fibrosis transmembrane conductance regulator gene. *J Biol Chem.* 1996; 271: 9947–54.
17. **Phylactides M, Rowntree R, Nuthall H, *et al.*** Evaluation of potential regulatory elements identified as DNase I hypersensitive sites in the CFTR gene. *Eur J Biochem.* 2002; 269: 553–9.
18. **Palstra RJ, Tolhuis B, Splinter E, *et al.*** The beta-globin nuclear compartment in development and erythroid differentiation. *Nat Genet.* 2003; 35: 190–4.
19. **Smith DJ, Nuthall HN, Majetti ME, *et al.*** Multiple potential intragenic regulatory elements in the CFTR gene. *Genomics.* 2000; 64: 90–6.
20. **Mouchel N, Henstra SA, McCarthy VA, *et al.*** HNF1α is involved in regulation of expression of the CFTR gene. *Biochem J.* 2004; 378: 909–18.
21. **McCarthy VA, Ott CJ, Phylactides M, *et al.*** Interaction of intestinal and pancreatic transcription factors in the regulation of CFTR gene expression. *Biochim Biophys Acta.* 2009; 1789: 709–18.
22. **Guenther MG, Young RA.** Transcription. Repressive transcription. *Science.* 2010; 329: 150–1.
23. **Rowntree R, Vassaux G, McDowell TL, *et al.*** An element in intron 1 of the CFTR gene augments intestinal expression *in vivo*. *Hum Mol Genet.* 2001; 11: 1455–64.
24. **Ott CJ, Suszko M, Blackledge NP, *et al.*** A complex intronic enhancer regulates expression of the CFTR gene by direct interaction with the promoter. *J Cell Mol Med.* 2009; 13: 680–92.
25. **Smith AN, Wardle CJ, Harris A.** Characterization of DNASE I hypersensitive sites in the 120kb 5' to the CFTR gene. *Biochem Biophys Res Commun.* 1995; 211: 274–81.
26. **Nuthall H, Vassaux G, Huxley C, *et al.*** Analysis of a DNAse I hypersensitive site located -20.9 kb upstream of the CFTR gene. *Eur J Bioch.* 1999; 266: 431–43.
27. **Gheldof N, Smith EM, Tabuchi TM, *et al.*** Cell-type-specific long-range looping interactions identify distant regulatory elements of the CFTR gene. *Nucleic Acids Res.* 2010; 38: 4325–36.
28. **Chung JH, Bell AC, Felsenfeld G.** Characterization of the chicken beta-globin insulator. *Proc Natl Acad Sci USA.* 1997; 94: 575–80.